Dynamics of Electron Holes in an Electron–Oxygen-Ion Plasma

B. Eliasson and P. K. Shukla

Institut für Theoretische Physik IV, Fakultät für Physik und Astronomie, Ruhr-Universität Bochum, D-44780 Bochum, Germany
(Received 12 March 2004; published 19 July 2004)

The dynamics of electron holes (EHs) in an electron–oxygen-ion plasma is studied by means of Vlasov simulations. It is found that EHs are attracted by ion density maxima but repelled by ion density minima. Standing EHs repel ions owing to the positive EH potential, creating an ion density cavity which ejects the EH, which propagates away from the cavity with a constant speed. On the other hand, propagating EHs can be trapped at ion density maxima. The results of our simulations will help in understanding the nonlinear dynamics of EHs in space and laboratory plasmas.

About a quarter century ago, Schamel [1] presented a theory for electron holes (EHs) [2–5], where a vortex distribution is assigned for the trapped electrons, and where the integration over the trapped and untrapped electrons in velocity space gives the electron number density as a function of the electrostatic potential, which is then calculated self-consistently from Poisson's equation. This model is suitable for analysis of the existence criteria for the EHs [1,4,5], and does also serve the purpose of providing initial conditions for controlled numerical simulations of EHs.

In laboratory experiments, the formation and coalescence of solitary EHs [6–9] and accelerated ion holes [10] have been observed. Observations of broad electrostatic noise (BEN) by the GEOTAIL [11] and FAST spacecrafts [12,13] in the auroral acceleration regions have revealed that BEN is connected to solitary electron Bernstein-Greene-Kruskal (BGK) modes or EHs. Recent observations by the WIND satellite in the Earth's bow shock also reveal localized structures with bipolar electric fields typical for electron BGK modes or holes [14–17]. The geomagnetic field-aligned bipolar electric field pulses associated with electron phase space holes have also been observed by the Polar and Cluster spacecrafts in the magnetosheath and at the Earth's magnetopause [18–20].

Even though the knowledge of *steady state EHs* has advanced significantly, little is known about the full dynamics of EHs that nonlinearly interact with ions in plasmas. Since EHs are associated with a positive electric potential, they repel ions. On the other hand, an ion density cavity (in the absence of EHs) is normally associated with a negative potential which in turn pushes electrons to neutralize the plasma. The positive potential of the EH and the negative potential of the ion density cavity are thus competing processes. Recent particle-in-cell (PIC) simulations [21] have shown a rapid decay of standing EHs into two or more nonisothermal ion-acoustic solitons (NIASs). In that numerical experiment, the electron-to-ion temperature ratio was chosen to 40 and the ion-to-electron mass ratio (m_i/m_e) to 100. For

these parameters, NIASs existed into which the EH could split. In the present investigation, however, with $T_e = T_i$ and $m_i/m_e = 29\,500$ (for oxygen ion), this channel of wave transformation is absent due to a lack of NIAs in this region, which would demand $T_e/T_i > 3.5$ (e.g., the second reference in [2]). Here T_e (T_i) is the electron (ion) temperature.

In this Letter, we study the fully nonlinear interaction between EHs and oxygen ions by means of a Vlasov simulation code which is based on a Fourier transform technique [22] where the electron and ion distribution functions are Fourier transformed in velocity space. The code solves the Vlasov equations for electrons and ions as well as Poisson's equation for the electrostatic field. The dimensionless Vlasov equation

$$\frac{\partial f_j}{\partial t} + v \frac{\partial f_j}{\partial x} - \frac{m_e q_j}{e m_j} \frac{\partial \phi}{\partial x} \frac{\partial f_j}{\partial v} = 0 \qquad (1)$$

describes the dynamics of the particle distribution f_j of the particle species j (where j equals e for electrons and i for ions), m_j is the mass, $q_e = -e$ ($q_i = e$) for electrons (ions), and e is the magnitude of the electron charge. The distribution function f_j is normalized by n_0/V_{Te}, where n_0 is the background electron number density, $V_{Te} = (T_e/m_e)^{1/2}$ is the electron thermal speed, T_e is the electron temperature, and m_e is the electron mass. The velocity v and the electrostatic potential ϕ are normalized by V_{Te} and T_e/e, respectively, whereas time and space variables are in units of the electron plasma period $\omega_p^{-1} = (4\pi n_0 e^2/m_e)^{-1/2}$ and the electron Debye radius $r_D = (T_e/4\pi n_0 e^2)^{1/2}$, respectively. The electrostatic potential is determined from Poisson's equation $\partial^2 \phi/\partial x^2 = N_e - N_i$, where the normalized (by n_0) particle number densities are given by $N_j = \int_{-\infty}^{\infty} f_j \, dv$.

The shape of the EH is not unique but is strongly dependent on the history of its creation. In order to investigate EHs numerically in a controlled manner, we shall use Schamel's solution of the stationary Vlasov-Poisson system in a comoving frame (i.e., moving with the EH) to construct initial conditions for our simulations. The Schamel solution is well behaved in the sense

that the solution for the distribution function is continuous and that it goes to a shifted Maxwellian distribution far away from the EH where the electric potential vanishes. Following Ref. [1], we prescribe solutions to the electron Vlasov equation in the form of distributions of free and trapped electrons. Integrating the untrapped and trapped electron distributions over velocity space, we obtain the electron density

$$N_e = e^{-M^2/2} \left\{ I(\phi) + \kappa\left(\frac{M^2}{2}, \phi\right) + \frac{2W_D[(-\beta\phi)^{1/2}]}{(\pi|\beta|)^{1/2}} \right\},$$
(2)

where $M = u/V_{Te}$ is the Mach number, u is the speed of the EH, and β is a trapping parameter [2]. Here, $I(\phi) = \exp(\phi)[1 - \mathrm{erf}(\phi^{1/2})]$, $\kappa(y, \phi) = (2/\sqrt{\pi}) \int_0^{\pi/2} y^{1/2} \times \cos(\alpha) \exp[-\phi\tan^2(\alpha) + y\cos^2(\alpha)]\mathrm{erf}[y^{1/2} \cos(\alpha)] \, d\alpha$, and $W_D(y) = \exp(-y^2) \int_0^y \exp(t^2) \, dt$. Poisson's equation, with N_e given by Eq. (2), is solved as a nonlinear boundary value problem, where ϕ is set to zero far away on each side of the EH. A central difference approximation is used for the second derivative in Poisson's equation, leading to a system of nonlinear equations, which is solved iteratively with (a slightly modified) Newton's method.

In Fig. 1, we have plotted the EH electric potential and electron number density for the case of a fixed ion background, viz. $N_i = 1$. We note that larger values of M and $|\beta|$ give smaller maxima ψ of the potential and less deep electron density minima, in agreement with Fig. 3(a) in Ref. [3]. The potentials obtained in Fig. 1 is used to construct the numerical initial conditions for the electron distribution function of EHs [3], to be used in our Vlasov simulations, including the ion dynamics. In Fig. 2, we show the time development of an EH, initially at rest. As the initial condition for the electron distribution function, we used the parameters $M = 0$ and $\beta = -0.7$ (the solid lines in Fig. 1), with a small local perturbation of the plasma near the EH. The perturbation consisted of a Maxwellian population of electrons added to the initial
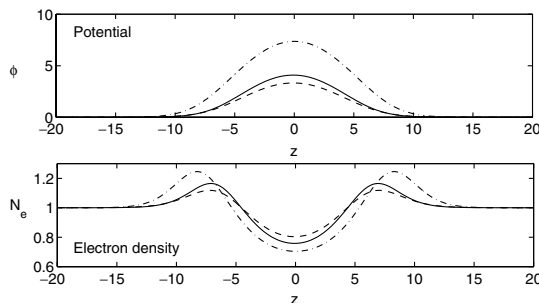
condition for the electron hole, with the same temperature as the background electrons and with the density perturbation of the form $\delta N_e = -0.008 \sinh(x/2)/\cosh^2(x/2)$. The most striking feature, seen at time $t \approx 130$, is that the EH "suddenly" starts moving in the negative x direction with a Mach number $M \approx 0.55$. (The direction of the propagation depends on the perturbation in the initial condition.) The transition seems to happen when the ion density has formed a deep enough cavity. When the EH has escaped the ion cavity, the ion density cavity continues to deepen and an electron density cavity is created at the same place, neutralizing the plasma. In Fig. 3, we have repeated the same numerical experiment as in Fig. 2, including the local perturbation of the plasma, but with $\beta = -0.5$, making the EH larger. In this case, the EH starts moving in the positive x direction at $t \approx 100$, also with a Mach number $M \approx 0.55$. For both the $\beta = -0.7$ and $\beta = -0.5$ cases, the potential maximum decreases slightly during the transition from standing to moving EHs, from $\psi = 4.5$ to $\psi = 3.8$ and from $\psi = 7.8$ to $\psi = 7.0$, respectively. For $M = 0.55$, the diagram in Fig. 3(a) in Ref. [3] predicts that the trapping parameter has changed to $\beta \approx -0.67$ and $\beta \approx -0.45$, respectively, for the two cases. We next analyze the distribution of energy in the system. The total energy is conserved exactly in the continuous system and to a high degree in our numerical simulations, and is distributed between kinetic energy of the particles and potential energy stored in the electric field [22,23]. In the upper panels of Fig. 4, we have plotted the potential energy $W_{\mathrm{pot}} = (1/2) \int E^2 \, dx$ of the system for the two simulation runs, as a function of time. We observe a gradual decrease of the potential energy until the transition time when the EH leaves the ion cavity and the potential energy

FIG. 1. The potential (upper panel) and the electron density (lower panel), associated with a standing electron hole ($M = 0$) with the trapping parameters $\beta = -0.7$ (solid lines) and $\beta = -0.5$ (dash-dotted lines), and a moving electron hole with $M = 0.5$ and $\beta = -0.7$ (dashed lines) in plasmas with fixed ion background ($N_i = 1$).
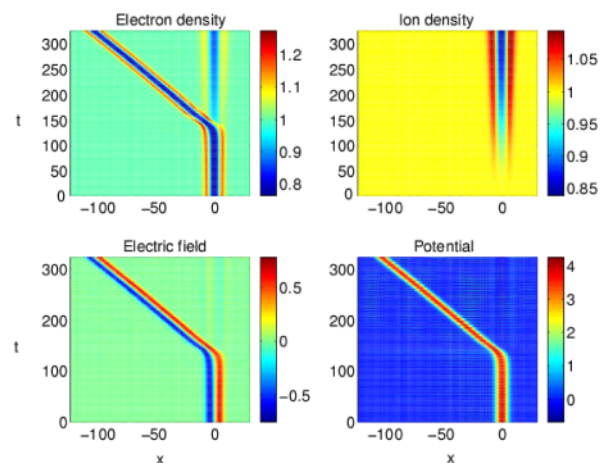

FIG. 2 (color online). The electron density (upper left panel), the ion density (upper right panel), the electric field (lower left panel) and the potential (lower right panel) of an initially stationary electron hole. The chosen trapping parameter is $\beta = -0.7$.
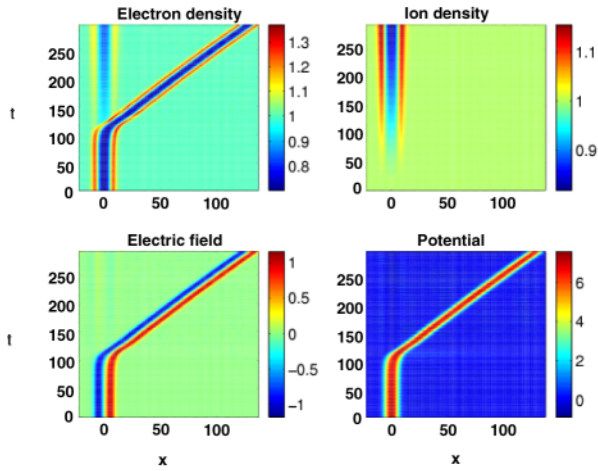
FIG. 3 (color online). The electron density (upper left panel), the ion density (upper right panel), the electric field (lower left panel) and the potential (lower right panel) of an initially stationary electron hole. The chosen trapping parameter is $\beta = -0.5$.

performs large fluctuations ($t \approx 130$ for the $\beta = -0.7$ case and $t \approx 100$ for the $\beta = -0.5$ case), whereafter the potential energy performs high-frequency oscillations attributed to propagating Langmuir waves excited in the transition, around a somewhat smaller constant W_{pot} attributed to the propagating EH bipolar electric field. The slow decrease of the potential energy in the initial phase indicates that the positive electrostatic potential of the EH accelerates the ions which leave the vicinity of the EH. In a homogeneous ion background, the single, steady-state EH is associated with a positive potential which
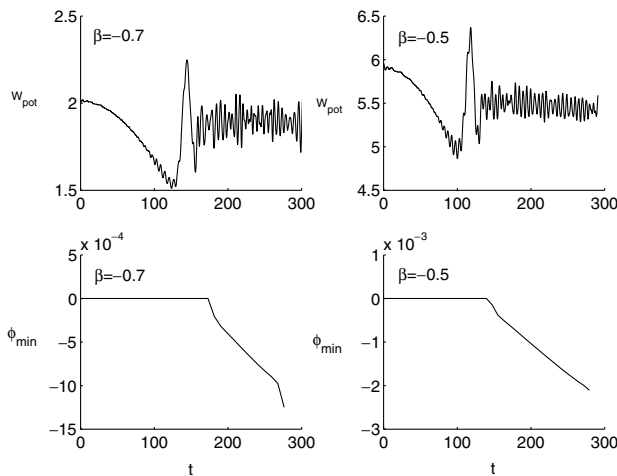
traps electrons. Since the positive potential of the EH and the negative potential of the ion cavity are competing processes, there could be a problem of the existence of a stationary EH if the ion density becomes deep enough. In our case, the EH remains stable but escapes the ion cavity. In the lower panels of Fig. 4, we have taken the ion density N_i obtained in our Vlasov simulations as an input to Poisson's equation, which we then solved with the electron density given by Eq. (2). The potential of the EH is normally positive everywhere when the ions are fixed background. In the presence of a local ion density cavity, the potential may have a slightly *negative* minimum, and at this point we prescribe a Maxwellian distribution for the untrapped electrons in the same manner as often done by Schamel [1,2,5]. We plotted the potential minimum $\phi_{\min}$ as a function of time, and found that at $t \approx 150$ a part of the potential becomes negative. It seems that the acceleration of the EH occurs at approximately the same time as a part of the potential for the theoretical model becomes negative. An alternative way of explaining accelerating EHs is as follows: The positive EH potential starts to reflect low energy ions giving rise to a local reduction of N_i. After a while, at the center of the EH, the condition $\phi''(x) = N_e(x) - N_i(x) < 0$ for x near zero is no longer met and the standing structure ceases to exist. Then the EH is accelerated such that a free ion component exists, giving rise to a free ion density $N_{if}(x)$ necessary for the maintenance of the inequality near the EH center. Figure 2 indicates that indeed $N_i(x) = N_{if}(x) \approx 1$.

Finally, we have studied interactions between two EHs with each other and with ions in a longer simulation; see Figs. 5 and 6 . The EH with $\beta = -0.5$ and $\beta = -0.7$ were initially placed at $x = -40$ and $x = 40$,

FIG. 4. The total potential energy $W_{\mathrm{pot}} = (1/2) \int E^2 dx$ as a function of time (upper panels) and the minimum of the electrostatic potential (lower panels) for $\beta = -0.7$ (left panels) and $\beta = -0.5$ (right panels), obtained from the model for a stationary electron hole in the presence of a varying ion density, where the ion density is obtained from the Vlasov simulations.
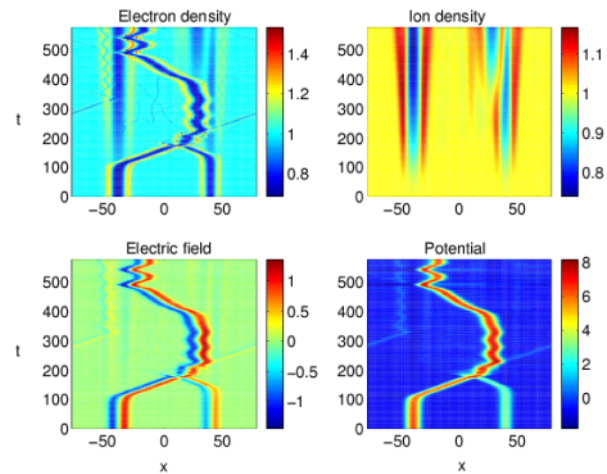

FIG. 5 (color online). The electron density (upper left panel), the ion density (upper right panel), the electric field (lower left panel), and the potential (lower right panel) of the two electron holes studied in Figs. 2–5. The trapping parameter $\beta = -0.5$ for the left EH initially placed at $x = -40$, and $\beta = -0.7$ for the right EH placed at $x = 40$.
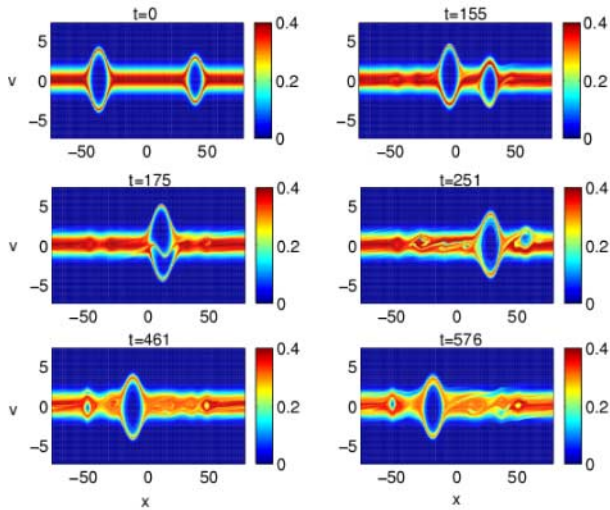
FIG. 6 (color online). The electron distribution for two electron holes at time $t = 0$ (upper left panel), $t = 155$ (upper right panel), $t = 175$ (middle left panel), $t = 251$ (middle right panel), $t = 461$ (lower left panel), and $t = 576$ (lower right panel). See the associated densities, etc., in Fig. 5. Initially, the left EH (placed at $x = -40$) has a trapping parameter $\beta = -0.5$, while the right EH (placed at $x = 40$) has a trapping parameter $\beta = -0.7$.

respectively. A local electron density perturbation was taken to be Maxwellian with the density $\delta N_e = -0.08\{\sinh[(x + 40)/2]/\cosh^2[(x + 40)/2] + \sinh[(x + 40)/2]/\cosh^2[(x + 40)/2]\}$, i.e., the same perturbations as in the single-hole cases, centered at the two electron holes. Here, the EHs also creates local ion density cavities, and after some time escapes the density cavities at the same times as in the single EH cases. This can clearly be seen in Fig. 5, where the two EHs start moving at $t \approx 100$ and $t \approx 130$, respectively. At $t \approx 170$, the two EHs collide and merge into a new EH (in accordance with the results of Ref. [11]), whereafter the single EH propagates slightly in the positive x direction, and becomes trapped at a local ion density maximum at $x \approx 30$; see the upper right panel of Fig. 5 for the ion density and the lower right panel for the EH potential. After $t \approx 400$, a new ion density cavity is created where the EH is centered, and at this time the EH is again accelerated in the negative x direction. At $t \approx 480$, the moving EH again encounters an ion density maximum located at $x \approx -30$, where the EH is trapped, performing large oscillations. The electron phase space density is depicted in Fig. 6, where we have the initial condition (upper left panel), the two EHs which now move (upper right panel), collisions between the two EHs (middle left panel), the newly created EH trapped at $x = 30$ (middle right panel), and the EH trapped at $x = -30$ (lower panels). We see that the EHs remain stable during the acceleration by ion density cavities; see also a movie of the EHs in Ref. [24].

To summarize, we have presented computer simulation studies of the nonlinear dynamics of electron holes interacting with ions in a Vlasov plasma. We find that EHs can be trapped by local ion density maxima, but are repelled by ion minima. A standing EH creates an ion density cavity which after some time ejects the EH, which propagates away from the ion hole with a speed close to half the electron thermal speed. Thus, standing large-amplitude EHs can exist only for a short period of time, before the EH is accelerated by the self-created ion density cavity. Our simulation results should help to understand the dynamics of large amplitude EHs that nonlinearly interact with ions in space and laboratory plasmas.

[1] H. Schamel, Phys. Scr. **20**, 336 (1979).
[2] H. Schamel, Plasma Phys. **13**, 491 (1971); **14**, 905 (1972).
[3] S. Bujarbarua and H. Schamel, J. Plasma Phys. **25**, 515 (1981).
[4] H. Schamel and S. Bujarbarua, Phys. Fluids **26**, 190 (1983).
[5] H. Schamel, Phys. Rep. **140**, 161 (1986); Phys. Plasmas **7**, 4831 (2000).
[6] K. Saeki et al., Phys. Rev. Lett. **42**, 501 (1979).
[7] H. L. Pécseli et al., Phys. Lett. **81**, 386A (1981); Phys. Scr. **29**, 241 (1984).
[8] H. L. Pécseli, Laser Part. Beams **5**, 211 (1987).
[9] G. Petraconi and H. S. Maciel, J. Phys. D **36**, 2798 (2003).
[10] C. Franck et al., Phys. Plasmas **8**, 4271 (2001).
[11] H. Matsumoto et al., Geophys. Res. Lett. **21**, 2915 (1994).
[12] R. E. Ergun et al., Phys. Rev. Lett. **81**, 826 (1998).
[13] R. E. Ergun et al., Geophys. Res. Lett. **25**, 2041 (1998); **25**, 2025 (1998).
[14] S. D. Bale et al., Geophys. Res. Lett. **25**, 2929 (1998).
[15] S. D. Bale et al., Astrophys. J. **575**, L25 (2002).
[16] M. Hoshino, Science **299**, 834 (2003)
[17] P. Guio and H. L. Pécseli, Geophys. Res. Lett. **31**, L03806/1-4 (2004).
[18] J. S. Pickett et al., Nonlinear Proc. Geophys. **9**, 1 (2002); **11**, 183 (2004).
[19] C. Cattel et al., Adv. Space Res. **28**, 1631 (2000).
[20] G. S. Lakhina et al., Nonlinear Proc. Geophys. **10**, 65 (2003).
[21] K. Saeki and H. Genma, Phys. Rev. Lett. **80**, 1224 (1998).
[22] B. Eliasson, J. Sci. Comput. **16**, 1 (2001); J. Comput. Phys. **190**, 501 (2003).
[23] R. Wangsness, *Electromagnetic Fields* (John Wiley & Sons, Inc., New York, 1986), 2nd ed.
[24] See EPAPS Document No. E-PRLTAO-93-052428 for a movie of the electron holes. A direct link to this document may be found in the online article's HTML reference section. The document may also be reached via the EPAPS homepage (http://www.aip.org/pubservs/ epaps.html) or from ftp.aip.org in the directory /epaps/. See the EPAPS homepage for more information.